J. Anat. (2006) **209**, pp69–78

Dynamic mechanics in the pig mandibular symphysis

G. E. J. Langenbach,[1] F. Zhang,[2] S. W. Herring,[3] T. M. G. J. van Eijden[1] and A. G. Hannam[2]

[1]*Department of Functional Anatomy, Academic Centre for Dentistry Amsterdam (ACTA), Universiteit van Amsterdam en Vrije Universiteit, The Netherlands*
[2]*Department of Oral Health Sciences, University of British Columbia, Vancouver, Canada*
[3]*Department of Orthodontics, University of Washington, Seattle, USA*

Abstract

During mastication, various biomechanical events occur at the mammalian jaw symphysis. Previously, these events have been studied in the static environment, or by direct recording of surface bone strains. Thus far, however, it has not been possible to demonstrate directly the forces and torques passing through the symphysis in association with dynamically changing muscle tensions. Therefore, we modified a previously published dynamic pig jaw model to predict the forces and torques at the symphysis, and related these to simulated masticatory muscle tensions, and bite, joint and food bolus forces. An artificial rigid joint was modelled at the symphysis, allowing measurements of the tri-axial forces and torques passing through it. The model successfully confirmed three previously postulated loading patterns at the symphysis. Dorsoventral shear occurred when the lower teeth hit the artificial food bolus. It was associated with balancing-side jaw adductor forces, and reaction forces from the working-side bite point. Medial transverse bending occurred during jaw opening, and was associated with bilateral tensions in the lateral pterygoid. Lateral transverse bending (wishboning) occurred at the late stage of the power stroke, and was associated with the actions of the deep and superficial masseters. The largest predicted force was dorsoventral shear force, and the largest torque was a 'wishboning' torque about the superoinferior axis. We suggest that dynamic modelling offers a new and powerful method for studying jaw biomechanics, especially when the parameters involved are difficult or impossible to measure *in vivo*.

Key words bone strain; chewing; masticatory system; modelling.

Introduction

The biomechanics of the mammalian mandibular symphysis have been studied extensively *in vivo* by strain gauge measurements in non-human primates (Hylander, 1979a, 1984, 1985), by electromyographic and cineradiographic recordings in non-human primates and mammals with unfused symphyses (Hylander & Johnson, 1994; Hylander et al. 1998, 2000, 2005; Lieberman & Crompton, 2000; Vinyard et al. 2006a,b) and by morphological analyses in a wide range of mammals (Daegling, 1993; Ravosa & Simons, 1994; Ravosa, 1996, 1999; Daegling & Jungers, 2000; Lieberman & Crompton, 2000). In addition, the relationship between symphyseal stress and strain has been estimated in a number of primate species (Vinyard & Ravosa, 1998).

In general, the unfused symphysis, by allowing independent inversion and eversion of the two halves of the mandible before and during the masticatory power stroke, enables the steep occluding surfaces of opposing teeth in some mammals to match during mastication (Kallen & Gans, 1972; Hylander, 1979b; Scapino, 1981; Oron & Crompton, 1985; Lieberman & Crompton, 2000). Fusion at the symphysis enables the effective use of all working- and balancing-side jaw adductor muscles to increase occlusal forces during unilateral chewing (Hylander, 1979b). Fusion strengthens and stiffens the jaw, reducing its risk of structural failure as a result of lateral transverse bending, and dorsoventral shear stresses occurring during unilateral mastication

Correspondence
Dr G. E. J. Langenbach, Department of Functional Anatomy, Academic Centre for Dentistry Amsterdam (ACTA), Meibergdreef 15, 1105 AZ Amsterdam, The Netherlands. F: +31 20 6911856; E: g.e.langenbach@amc.uva.nl

Accepted for publication *14 March 2006*

(Hylander, 1984; Ravosa & Hylander, 1993; Ravosa & Simons, 1994; Ravosa, 1996; Hylander et al. 2000, 2005; Vinyard et al. 2006a,b).

In mammals with fused symphyses, high stresses and strains can occur during the generation of unilateral occlusal forces (van Eijden, 2000). Dorsoventral shear is created by the upward component of the balancing-side jaw-muscle force, and the downward component of the bite point reaction force during unilateral biting (Hylander, 1979a, 1984, 1985). During chewing, lateral transverse bending (wishboning) occurs at the end of the power stroke, i.e. after the initial occurrence of maximum intercuspation, and is associated with the late peak activity of the balancing-side deep masseter coupled with the rapid decline in the activity of the balancing-side medial pterygoid and superficial masseter (Hylander & Johnson, 1994). Additional oppositely directed lateral force components originating from the working-side superficial masseter and the oppositely directed lateral component of the working-side bite point reaction force may also contribute (Hylander, 1984, 1985; Hylander & Johnson, 1994). Wishboning produces primary compressive stress and strain on the labial aspect and primary tensile stress and strain on the lingual aspect of the symphysis (Hylander, 1984, 1985). A third loading pattern is medial transverse bending, which occurs during jaw opening and has been postulated to be caused mainly by the bilateral contraction of the lateral pterygoid muscles, producing a reversed wishboning effect (Hylander, 1984, 1985). This form of loading causes compression on the lingual aspect and tension on the labial aspect of the symphysis.

These *in vivo* studies, although measuring dynamic strains, have limitations. One cannot sample surface strains at more than a few sites in the mandible without compromising the structural and functional integrity of the masticatory system (Daegling & Hylander, 2000). In addition, the analysis of such strain data is not entirely unambiguous, as they are interpreted in light of idealized morphological representations of the tissues involved. A shortcoming of previous biomechanical analyses and stress and strain estimations is their consideration in static situations (see, for example, Vinyard & Ravosa, 1998). The concerted influence of the various muscle forces, the occlusal forces and reaction forces at the two joints on the symphyseal forces and torques during dynamic conditions remains largely undetermined.

Dynamic jaw models have been utilized to study jaw musculoskeletal mechanics in humans (Koolstra & van Eijden, 1995, 1996, 2005; Hannam et al. 1997; Langenbach & Hannam, 1999; Peck et al. 2000; Koolstra, 2002; Hansma et al. 2006) and in pigs (Langenbach et al. 2002). These dynamic jaw models incorporate many structural and functional data. Using predefined muscle activity patterns these models have the ability to predict jaw motions, muscle tensions and reaction forces in real time, parameters which are presently impossible to record *in vivo*. Dynamic models thus have the unique potential to estimate internal forces and torques induced by multiple, changing muscle tensions.

In the current study, a previously published (Langenbach et al. 2002) three-dimensional dynamic model of the pig jaw system was used to simulate chewing. A modification of the model made it possible to predict the tri-axial dynamic forces, and torques passing through the symphysis as a result of muscle tensions and concomitantly generated resultant forces. It was hypothesized that these changing symphyseal forces and torques could be categorized into three loading patterns, i.e. dorsoventral shearing, wishboning and medial transverse bending. It was further hypothesized that each of these symphysial loading patterns could be linked to concurrent muscle tensions according to previously published hypotheses.

Methods

Model generation

The original model of the pig jaw has been reported elsewhere (Langenbach et al. 2002) and was designed with a commercial software package (ADAMS 10.0, Automatic Dynamic Analysis of Mechanical Systems; Mechanical Dynamics Inc., Ann Arbor, MI, USA). Briefly, the model (Fig. 1) incorporated the muscular and skeletal morphology from a female miniature pig (*Sus scrofa*, 8 months old). Computer tomography (CT) with a calibration phantom was performed to obtain its skeletal structure and mass properties (Zhang et al. 2001). Muscle cross-sectional sizes, lines of actions and attachment sites were obtained through magnetic resonance imaging. Three lines of action were assigned to the temporalis muscle (anterior, middle and posterior), two to the masseter (superficial and deep), and one to each medial pterygoid, lateral pterygoid and digastric muscle. Each muscle model included fibre and tendon

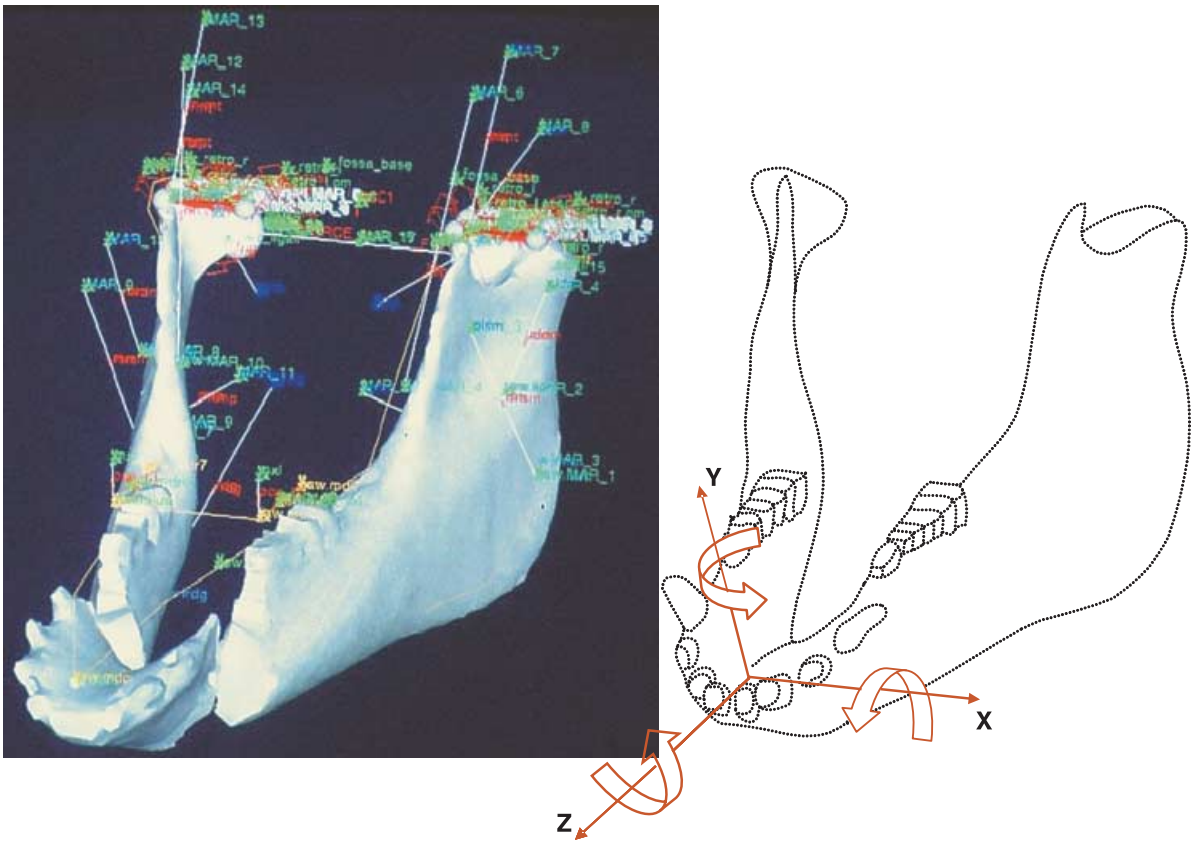

Fig. 1 Oblique view of the ADAMS wireframe dynamic model (left) and the conventions used to express symphyseal forces and torques (right). Muscle action lines are described elsewhere (Langenbach & Hannam, 1999; Langenbach et al. 2002). The rigid joint linking the two halves of the mandible is not indicated but is located at the centre of the symphysis approximately at the origin of the axes shown at the right. Forces exerted by the working-side corpus on the balancing-side corpus are positive when they are in the same direction as the axes. Arrows around each axis indicate the directions of positive torques exerted by the working-side corpus on the balancing-side.

components. The fibre/tendon length ratios were defined according to published data (Herring & Scapino, 1973; Anapol & Herring, 1989).

Muscle function was simulated as described in detail previously (Langenbach & Hannam, 1999; Langenbach et al. 2002). In brief, motion of the mandible was produced by active muscle tensions. Each active muscle tension was determined by the product of the muscle's cross-sectional area, a constant of 40 N cm^{-2} (Weijs & Hillen, 1985) and a specified level of activation for that time period (0–1, where unity represents 100% activation). This value, expressed in Newtons (N), was scaled according to the muscle's instantaneous length and shortening velocity by means of length–tension and velocity–tension curves (Zajac, 1989). Any passive muscle tension induced by damping or stretch was then added to this active tension. Passive stretch tensions were only present for lengths beyond the optimal muscle length, taken as the muscle length at an inter-incisal distance of 30 mm. For the masseter, this results in a situation similar to what was found by Anapol & Herring (1989).

To simulate chewing, the model was driven with muscle activity patterns based on electromyographic data, recorded during chewing from the same animal, also providing the skeletal and muscular data for the reconstruction of the model. Recordings made unilaterally for some muscles could be extrapolated to the other side by examining another chewing cycle, as the pig chews alternately right and left. For the temporalis, activity patterns were averaged measurements described previously for pig mastication (Herring & Scapino, 1973). Jaw motions predicted by the model were expected to comply with ranges found for opening, laterodeviation and timing of the various chewing cycle phases (Herring & Scapino, 1973; Herring, 1976). During closing a modelled food bolus (60 N) had to be completed compressed, without generating occlusal

forces exceeding the 100 N after complete bolus compression. When the chewing cycle did not meet all the above criteria, one or more of the initial activity patterns were altered by changing the amplitudes, not the timing (see also Langenbach et al. 2002).

Segmentation of the mandible from CT images has been depicted elsewhere (Zhang et al. 2001). To generate a symphyseal region, the reconstructed mandible was split midsagittally. Each half of the mandible was saved as a separate file for calculation of mass properties with a custom-made program (Calimage, The University of British Columbia, Vancouver, BC, Canada). The model thus consisted of two independent rigid bodies representing the two corpora of the mandible. These were linked with a rigid pin-joint placed at the centre of the symphyseal region and orientated orthogonally to the dental occlusal plane (Fig. 1). The jaw's motions relative to the cranium were shaped by the active and passive muscle tensions, gravity, the reaction forces at the temporomandibular joints and the dental occlusion, and food bolus resistance. Condylar guidance was simulated with a horizontal plane, resembling the joint morphology. Under loading, the condylar centre could indent this plane (the reaction force increased exponentially to reach 1000 N at 0.25-mm compression), but rotations and translations on the plane were frictionless. All muscle actuators linked the mandible to the cranium.

The locations of three mandibular bite points [buccal cusp tips of both mandibular fourth premolars (DP4) and of the mid-incisor] in the dental arch were obtained from the three-dimensional CT reconstruction of the mandible. Reaction forces at these bite points were assumed to be perpendicular to the occlusal plane, and were generated when the jaw reached the dental intercuspal position, where the interocclusal contact force at each bite point increased exponentially to reach 2000 N with 0.25-mm interocclusal compression. The model was designed to accommodate a food bolus on the working-side at the DP4 bite point. The bolus had a compressive resistance that depended on its thickness (equivalent to the distance separating the dental arches at that location). It was 3.0 mm thick, and its resistance increased over the first 1.5 mm of compression, to reach a maximum of 60 N. Bite forces of less than 60 N (or of insufficient duration) resulted in incomplete bolus compression. Forces of greater than 60 N (and of sufficient duration) caused an interocclusal contact force.

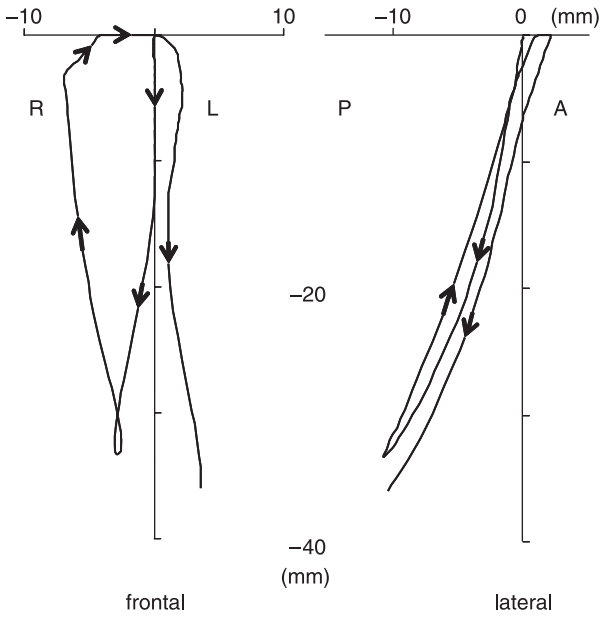

Fig. 2 Frontal (left) and lateral (right) view of the incisor point motion during a simulated right-sided chewing cycle. Arrows indicate the direction of motion, including the next stroke to the contralateral side. See text for full description. R, right; L, left; P, posterior; A, anterior.

Simulations

In the present study, we analysed the simulation for one right-sided chewing cycle over 0.5 s. Output predictions included incisal point movement in vertical, horizontal and anteroposterior dimensions, tensions of the 16 jaw muscles, reaction forces at the working-side bite points, reaction forces at the temporomandibular joints, and tri-axial forces and torques passing through the symphysis. All were time-related dynamic measurements. The conventions used to express symphyseal forces and torques are illustrated in Fig. 1.

Results

Incisor point motion

The predicted jaw motion (Fig. 2) was reasonably similar to previously published characteristics of pig chewing (Herring & Scapino, 1973; Herring, 1976). Viewed frontally, jaw opening began in the midline. After the first 10 mm of gape, the jaw deviated from the midline towards the working-side. Maximum opening (33 mm) was followed by fast closure of the jaw combined with a further lateral deviation (7 mm) of the jaw. When the artificial food bolus was reached, the jaw moved back

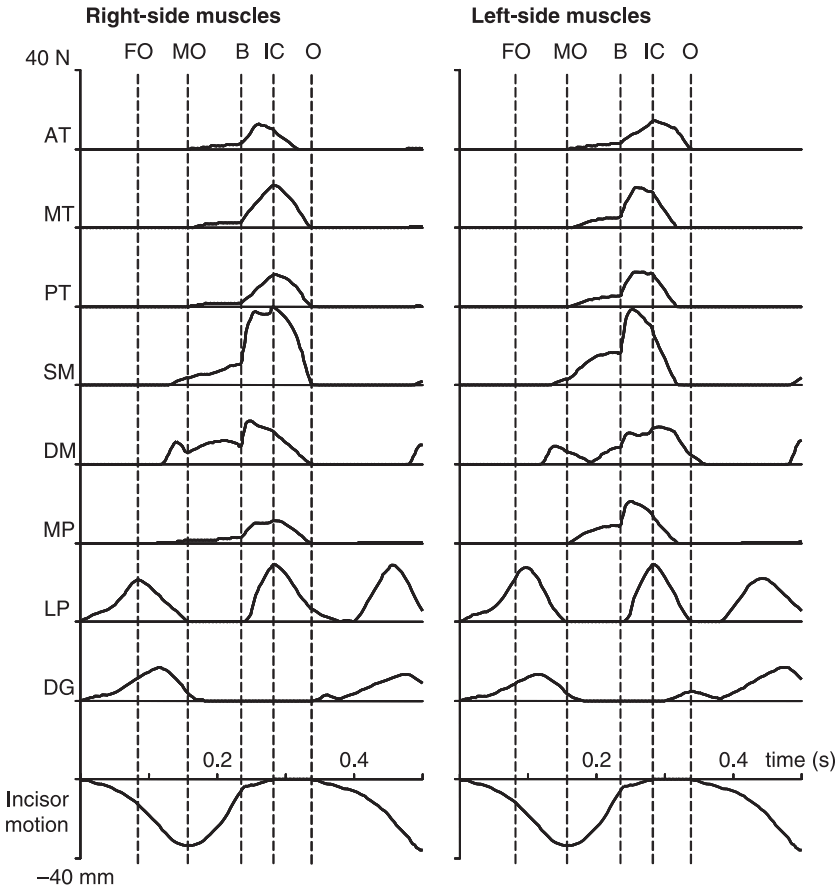

Fig. 3 Muscle tensions expressed in time during simulated right-sided chewing. Data are shown for the working- and balancing-sided muscles. The lowest curve is the corresponding incisor point motion in the vertical dimension. The dotted lines in each figure (from left to right) represent fast jaw opening (FO), maximum jaw opening (MO), onset of bolus crush (B), the onset of tooth-to-tooth contact in intercuspation (IC) and start of jaw opening (O). AT, anterior temporalis; MT, middle temporalis; PT, posterior temporalis; SM, superficial masseter; DM, deep masseter; MP, medial pterygoid; LP, lateral pterygoid; DG, digastric.

to the midline, and closed slowly. Vertical jaw motion stopped when the teeth came into contact, resulting in a horizontal slide through the midline towards the balancing-side. The right-sided cycle took 0.33 s before the next cycle commenced, which started on the balancing side of the midline.

Muscle tensions

Tensions of the 16 muscles expressed as a function of time for the simulated chewing stroke are presented in Fig. 3. Activation of the lateral pterygoid and digastric muscles on both sides initiated the cycle. The lateral pterygoid muscle on the working-side reached its peak tension slightly earlier (about 0.02 s) than its balancing-side counterpart, and clearly earlier than both digastrics on both sides. Peak lateral pterygoid tension coincided with the start of fast opening (the first vertical line in Fig. 3). When the jaw reached maximum gape (33 mm), the tension of the lateral pterygoid muscles reduced to zero. The digastric muscle tensions also disappeared at the beginning of the closing phase.

During jaw opening, passive tensions were produced in both masseter portions and the medial pterygoid. These passive tensions turned into active tensions at the beginning of the closing phase (MO line in Fig. 3). When the teeth hit the artificial bolus (B line in Fig. 3), all adductor muscles were active, soon followed by the lateral pterygoid muscles. On the working-side, whereas the deep masseter reached maximum tension immediately after the teeth began to crush the bolus, other adductors and lateral pterygoid muscle reached their maximum tensions later, i.e. when the bolus was almost completely crushed, and the lower teeth contacted the upper teeth (IC line in Fig. 3). On the balancing-side, the middle and posterior temporalis muscles, superficial masseter, and medial pterygoid muscle all reached their maximum tensions earlier than the deep masseter and lateral pterygoid. The last two of these muscles reached their maximum tensions late, i.e. during the intercuspal slide to the midline.

Forces at the artificial food bolus, tooth and joints

Forces expressed in time at the food bolus, working-side tooth point (DP4), and working-side and balancing-side

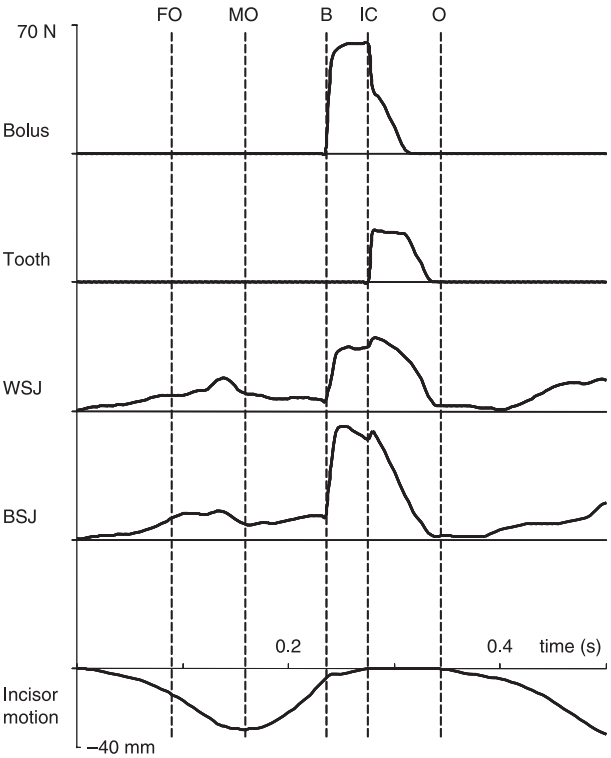

Fig. 4 Predicted forces expressed in time. They include bolus, working-side bite point (tooth), working-side (WSJ) and balancing-side temporomandibular joint (BSJ) forces. The lowest curve is the corresponding incisor point motion in the vertical dimension. FO, start of fast opening; MO, maximum jaw opening; B, onset of bolus crush; IC, onset of tooth-to-tooth contact in intercuspation; O, onset of jaw opening.

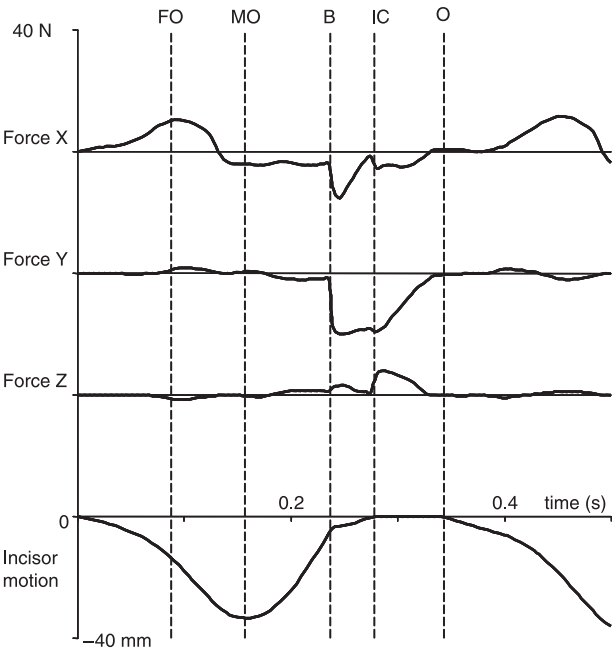

Fig. 5 Tri-axial symphyseal forces expressed in time. The lowest curve is the corresponding incisor point motion in the vertical dimension. FO, start of fast opening; MO, maximum jaw opening; B, onset of bolus crush; IC, onset of tooth-to-tooth contact in intercuspation; O, onset of jaw opening.

temporomandibular joints are illustrated in Fig. 4. The reaction force at the food bolus began to increase when struck by the lower teeth, increased steeply in about 0.01 s and after a slower phase of 0.02 s reached its maximum; this peak force continued for about 0.03 s, then decreased sharply when intercuspation occurred. Tooth force was produced and reached its maximum immediately after the food bolus was completely compressed and tooth contact was made. Reaction forces at both joints commenced with opening, and reached small peaks just before maximum gape. These forces increased steeply when the tooth hit the artificial bolus. The balancing-side joint force reached maximum shortly after, and the working-side joint force reached maximum after initial tooth contact occurred. All these forces disappeared before the next cycle began.

Tri-axial symphyseal forces and torques

The tri-axial symphyseal forces expressed in time are demonstrated in Fig. 5. During jaw opening, the symphysis underwent compression (11 N) along its transverse *x*-axis (i.e. the balancing-side corpus was compressed by the working-side corpus in the occlusal plane; cf. Fig. 1). This compression coincided with peak tension in the lateral pterygoid and digastric muscles (cf. Fig. 3). When the jaw reached maximum opening, symphyseal tension (4 N) was induced (i.e. the balancing-side corpus was tensed by the working-side corpus; cf. Fig. 1), and stayed almost constant until the lower teeth hit the artificial bolus. This tension reached a maximum (15 N) during the early stage of bolus crushing and then decreased. These effects were related to peak active tension in the closing muscles, most notably the superficial and deep masseters (cf. Fig. 3).

A negative symphyseal shear force began along the superoinferior *y*-axis when the food bolus was hit, and increased steeply (20 N). This shear was related to the reaction force applied on the working-side DP4, which tended to lower the working-side corpus, and jaw adductor forces on the balancing-side, which lifted the balancing-side corpus. The shear force continued until the bolus was completely crushed, and began to decrease when the lower teeth made contact with the upper teeth (cf. Fig. 4).

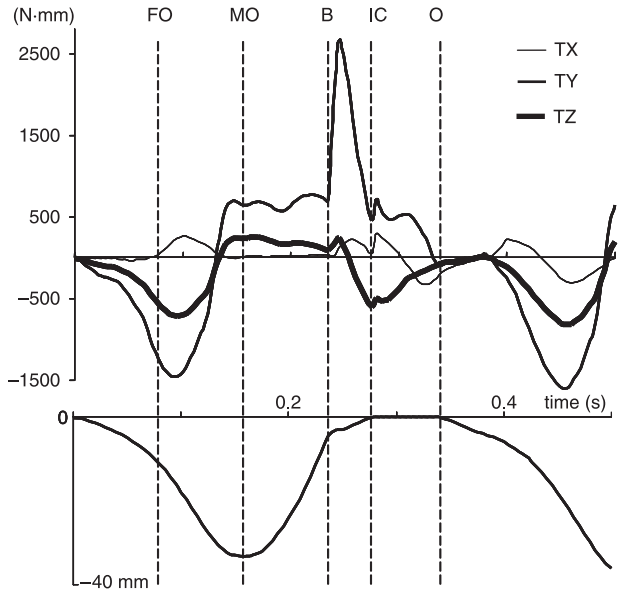

Fig. 6 Tri-axial symphyseal torques expressed in time. The lowest curve is the corresponding incisor point motion in the vertical dimension. TX, TY and TZ are torques about the *x*-, *y*- and z-axes, respectively. FO, start of fast opening; MO, maximum jaw opening; B, onset of bolus crush; IC, onset of tooth-to-tooth contact in intercuspation; O, onset of jaw opening.

A small shear force (up to 7 N) along the anteroposterior *z*-axis was probably caused by different timing in the temporalis, medial pterygoid and masseter muscles, and as a possible result of muscle forces on the working-side exceeding those on the balancing-side after tooth contact commenced (cf. Fig. 3).

The symphyseal torques around the three axes are shown in Fig. 6. Two small positive torques (approximately 250 N·mm) occurred around the transverse *x*-axis. The first occurred at the start of the fast opening phase at about 0.1 s. The balancing-side jaw tended to be twisted more than the working-side due to the balancing-side lateral pterygoid tension exceeding that of the working-side lateral pterygoid, so the twisting force exerted on the balancing-side symphysis by the working-side was in a clockwise direction (cf. Fig. 1). The second positive torque commenced with the onset of bolus crushing, reached a peak after the bolus was completely crushed, and was due to the bolus reaction force coupling with the balancing-side jaw lifting forces.

The torques around the *y*-axis were induced by twisting related to the transverse bending of the mandibular corpora. The initial negative torque was associated with the activity of the two jaw openers when the medial transverse bending occurred. The magnitude of this torque was about –1500 N·mm. This torque changed direction when passive tension of superficial and deep masseter (wishboning) began to increase and quickly reached about 750 N·mm the moment the jaw reached maximum opening. The torque stayed almost constant until the lower teeth began to crush the food bolus. It then rose steeply to a maximum of over 2500 N·mm during the first one-third of the bolus crushing phase, followed by a sharp drop in magnitude. The peak torque coincided with the maximum tensions of the superficial and deep masseter muscles on both sides, and the peak bolus reaction force. The torque reduced to about 500 N·mm after tooth contact occurred, and started to decline before the next cycle (cf. Fig. 3).

The torques around the *z*-axis were the results of asymmetrical jaw opening and closing muscle forces, which tended to turn the mandible about its anteroposterior *z*-axis. They coincided with the two transverse torques, and were the consequences of the same muscle contraction patterns.

Discussion

The model

The plausibility of a pig dynamic model has been demonstrated in another study (Langenbach et al. 2002), i.e. the predicted jaw motion complied with several other previously published characteristics of pig chewing. However, the model simplified some of the pig's musculoskeletal properties. For example, the pig masseter is large, and shows differential activities (Herring et al. 1989), yet here we devide it only into two regions (superficial and deep) because the detailed cross-sectional data for smaller components were unknown. In addition, the definition of a pure vertical directed bite force is not fully realistic as the occlusal surface is not entirely smooth. Furthermore, only one chew in one animal was modelled, while the variation in chewing cycles can be large within and between animals. Alterations in the activity patterns, or in any antomical or functional features will have their influence on the symphyseal force and torque estimations. Nonwithstanding all these limitations, the resulting chewing cycle can be considered as normal according to various motion parameters (Langenbach et al. 2002). Therefore, the assumption can be made also that the

predicted symphyseal biomechanics can be considered to be normal, or at least within the range of possible forces generated during chewing.

The model assumed the mandible consisted of two rigid structures linked by a fixed joint placed centrally at the mandibular symphysis. Conceptually, it was equivalent to two rigid beams (independent of their cross-sectional forms) linked at a point through which all forces and torques were transmitted. Yet, this approach cannot predict the stress and strain within the corpora or at their surfaces. In addition, the interpretation of direct measurements of surface strain data at the symphysis and the comparison of such strains with the current predictions of symphyseal forces and torques is complicated as the symphyseal surface is large and irregular, suggesting regionally variable mechanical properties. However, the model was capable of revealing the environment in which the symphysis might work. The assumption was that the design of the corpora provides a high degree of rigidity in the intact animal; thus, any symphyseal link, whatever its form, would have to be designed to cope with the resultant total forces and torques demonstrated by the model.

A clear advantage of the current approach is the dynamic character of the simulations. Static models are valuable for the detailed examination of a specific situation. The concerted influence of changing forces during, for instance, chewing and generated by different tissues and at numerous sites can only be examined in a dynamic fashion. Although the current method is a reasonable approach to estimate internal bone forces and torques, a further development in modelling bone deformations is necessary. In this, finite-element analysis provides a better overall view of the possible forces experienced by the modelled tissues. However, these models are unable to depict satisfactorily the appropriate boundary conditions, such as the various muscle tensions involved. In this, dynamic modelling in combination with finite element analysis and detailed reconstruction of the bone architecture (Koolstra & van Eijden, 2005; van Eijden et al. 2006) can provide a valuable tool in the assessment of cortical and trabecular bone loading patterns due to functional muscle tensions.

Predicted dorsoventral shear

In vivo studies of monkey mandibles indicate that the mandibular symphysis is sheared dorsoventrally during unilateral molar biting. It is created by the upward component of the balancing-side jaw-muscle force, and the downward component of the bite point reaction force during unilateral biting (Hylander, 1979a, 1984, 1985). The present results suggest that if pigs also evince unilateral biting, then dorsoventral shear will also be one of the most important dynamic loads in the pig jaw symphysis. This shear force starts to increase when the reaction force on the lower teeth couples with balancing-side jaw adductor forces (Fig. 5), a mechanism similar to that found in monkeys. The prediction agrees with the hypothesis that the pig symphysis undergoes loading like that in non-human primates. However, it is important to note that unilateral molar biting may not always occur and that pigs regularly have a bilateral occlusion as well. If it does, then the magnitude of this shear force would be the largest in the symphysis. This load couples with the parasagittal bending of the mandibular body, a main loading element of the mandibular corpus (Hylander, 1979b; van Eijden, 2000), owing to muscle and bite forces. Fusion assists in resisting this large shearing force, but a large symphyseal cross-sectional area would also be necessary (Hylander, 1984; Daegling, 1989; van Eijden, 2000).

Predicted lateral transverse bending or wishboning

In vivo studies of monkey mandibles indicate that the mandibular symphysis is wishboned during unilateral molar biting. This occurs at the very end of the power stroke, i.e. after the initial occurrence of maximum intercuspation, and is associated with the late peak activity of the balancing-side deep masseter coupled with the rapid decline in the activity of the balancing-side medial pterygoid and superficial masseter (Hylander & Johnson, 1994). Although the lateral component of balancing-side deep masseter is considered to be the primary masticatory muscle force associated with symphyseal wishboning, residual activity from the working-side superficial masseter and the oppositely directed lateral component of the working-side bite point reaction force may also contribute (Hylander, 1984, 1985; Hylander & Johnson, 1994). This latter factor was not included in the current model and would increase the predicted wishboning effect. Nevertheless, lateral transverse bending was predicted as the most important loading regime because the predicted maximum torque was well beyond the largest torque during

medial transverse bending (Fig. 6), exceeding 2500 N·mm. In addition to the masseter contribution, concurrent actions of the genial muscles could have enhanced the wishboning effect, but these muscles were not included in the model. Except for the muscular factor, the model associated wishboning with bite and articular forces. As the artificial food bolus was crushed in a supero-medial direction by the lower tooth, the reaction force from the food bolus had a laterally directed component. Because the pig has a relatively flat articular fossa with a medio-lateral slope, wishboning here would also have been influenced by joint reaction forces on both sides. Again, it is important to note that if the occlusal contact is bilateral rather than unilateral, these torques would be modified. Indeed, preliminary *in vivo* strain gauge data suggest that lateral transverse bending may not be the major regime in pigs, as opposed to monkeys (S. W. Herring and K. L. Rafferty, unpublished data).

Predicted medial transverse bending

In vivo studies of monkey mandibles indicate that the mandibular symphysis is bent transversely and medially. This medial transverse bending occurs in the opening phase and has been considered to be the result of the bilateral contraction of the lateral pterygoid muscles (Hylander, 1984, 1985). The dynamic model predicted medial transverse bending associated with pig jaw opening. The initial bending was expressed as compression, started with jaw opening and reached a maximum when the lateral pterygoid muscles arrived at their peak tensions (Figs 3 and 5). The digastric muscles did not contribute to medial transverse bending owing to their anterio-posterior orientation, as they mainly open and retrude the jaw. Medial transverse bending produces the second largest torque (Fig. 6), which is relatively large as compared with *in vivo* data for strains. This might be related to a difference in the site of measurement. The current approach cannot predict the stress and strain at the bone surface, where the strains are normally recorded.

As a curved beam, the mandibular symphysis, especially its lingual side, undergoes the highest stress during wishboning (Hylander, 1985). To counter this wishboning torque effectively, not only the size, but also the shape and cortical bone distribution of the pig jaw symphysis are important (Hylander, 1984; Daegling, 2001). A large cross-sectional moment of inertia with respect to the axis perpendicular to the bending plane is required (Hylander, 1985; van Eijden, 2000). This can be accomplished by a horizontally orientated symphysis as seen in pigs. The results from this study offer evidence for the hypothesis that the pig jaw symphyseal size and orientation are adaptations to counter concentrated wishboning stresses during function.

In conclusion, the method outlined here enables the detailed study of forces and torques travelling through the mandible as a consequence of the changing forces produced by the various jaw muscles, bite points and joints. *In vivo* studies provide the necessary validation of these results, but are limited to specific experimental situations or limited in their amount of concurrent measurements. Combining dynamic modelling with finite-element analysis (Koolstra & van Eijden, 2005) can be a valuable tool in the estimation of bone loading patterns resulting from functional use of the mandible.

Acknowledgements

This study was financially supported by the MRC (Canada) and the NIH (PHS award DE 11962). We thank Joy Scott for her assistance in data analysis. We are grateful to Jan Harm Koolstra for his thoughtful comments on this manuscript.

References

Anapol F, Herring SW (1989) Length–tension relationships of masseter and digastric muscles of miniature swine during ontogeny. *J Exp Biol* **143**, 1–16.

Daegling DJ (1989) Biomechanics of cross-sectional size and shape in the hominoid mandibular corpus. *Am J Phys Anthropol* **80**, 91–106.

Daegling DJ (1993) Shape variation in the mandibular symphysis of apes: an application of a median axis method. *Am J Phys Anthropol* **91**, 505–516.

Daegling DJ, Hylander WL (2000) Experimental observation, theoretical models, and biomechanical inference in the study of mandibular form. *Am J Phys Anthropol* **112**, 541–551.

Daegling DJ, Jungers WL (2000) Elliptical fourier analysis of symphyseal shape in great ape mandibles. *J Human Evol* **39**, 107–122.

Daegling DJ (2001) Biomechanical scaling of the hominoid mandibular symphysis. *J Morph* **250**, 12–23.

van Eijden TMGJ (2000) Biomechanics of the mandible. *Crit Rev Oral Biol Med* **11**, 123–136.

van Eijden TMGJ, van der Helm PN, van Ruijven LJ, Mulder L (2006) Structural and mechanical properties of mandibular condylar bone. *J Dent Res* **85**, 33–37.

Hannam AG, Langenbach GEJ, Peck CC (1997) Computer simulations of jaw biomechanics. In *Science and Practice of Occlusion* (ed. McNeill C), pp. 187–194. Carol Stream: Quintessence.

Hansma HJ, Langenbach GEJ, Koolstra JH, van Eijden TMGJ (2006) Passive resistance increases differentially in various jaw displacement directions. *J Dent* in press. doi: 10.1016/j.dent.2005.11.005

Herring SW, Scapino RP (1973) Physiology of feeding in miniature pigs. *J Morph* **141**, 427–460.

Herring SW (1976) The dynamics of mastication in pigs. *Arch Oral Biol* **21**, 473–480.

Herring SW, Wineski LE, Anapol FC (1989) Neural organization of the masseter muscle in the pig. *J Comp Neurol* **280**, 563–576.

Hylander WL (1979a) Mandibular function in *Galago crassicaudatus* and *Macaca fascicularis*: an *in vivo* approach to stress analysis of the mandible. *J Morph* **159**, 253–296.

Hylander WL (1979b) The functional significance of primate mandibular form. *J Morph* **160**, 223–240.

Hylander WL (1984) Stress and strain in the mandibular symphysis of primates: a test of competing hypotheses. *Am J Phys Anthropol* **64**, 1–46.

Hylander WL (1985) Mandibular function and biomechanical stress and scaling. *Am J Zool* **25**, 315–330.

Hylander WL, Johnson KR (1994) Jaw muscle function and wishboning of the mandible during mastication in macaques and baboons. *Am J Phys Anthropol* **94**, 523–547.

Hylander WL, Ravosa MJ, Ross CF, Johnson KR (1998) Mandibular corpus strain in primates: further evidence for a functional link between symphyseal fusion and jaw-adductor muscle force. *Am J Phys Anthropol* **107**, 257–271.

Hylander WL, Ravosa MJ, Ross CF, Wall CE, Johnson KR (2000) Symphyseal fusion and jaw-adductor muscle force: an EMG study. *Am J Phys Anthropol* **112**, 469–492.

Hylander WL, Wall CE, Vinyard CJ, et al. (2005) Temporalis function in anthropoids and strepsirrhines: an EMG study. *Am J Phys Anthropol* **128**, 35–56.

Kallen FC, Gans C (1972) Mastication in the little brown bat, *Myotis lucifugus*. *J Morph* **136**, 385–420.

Koolstra JH, van Eijden TMGJ (1995) Biomechanical analysis of jaw-closing movements. *J Dent Res* **74**, 1564–1570.

Koolstra JH, van Eijden TMGJ (1996) Influence of the dynamical properties of the human masticatory muscles on jaw closing movements. *Eur J Morph* **34**, 11–18.

Koolstra JH (2002) Dynamics of the human masticatory system. *Crit Rev Oral Biol Med* **13**, 368–380.

Koolstra JH, van Eijden TMGJ (2005) Combined finite-element and rigid-body analysis of human jaw joint dynamics. *J Biomech* **38**, 2431–2439.

Langenbach GEJ, Hannam AG (1999) The role of passive muscle tensions in a three-dimensional dynamic model of the human jaw. *Arch Oral Biol* **44**, 557–573.

Langenbach GEJ, Zhang F, Herring SW, Hannam AG (2002) Modelling the masticatory biomechanics of a pig. *J Anat* **201**, 383–393.

Lieberman DE, Crompton AW (2000) Why fuse the mandibular symphysis? A comparative analysis. *Am J Phys Anthropol* **112**, 517–540.

Oron U, Crompton AW (1985) A cineradiographic and electromyographic study of mastication in *Tenrec ecaudatus*. *J Morph* **185**, 155–182.

Peck CC, Langenbach GEJ, Hannam AG (2000) Dynamic simulation of muscle and articular properties during human wide jaw opening. *Arch Oral Biol* **45**, 963–982.

Ravosa MJ, Hylander WL (1993) Functional significance of an ossified mandibular symphysis: a reply. *Am J Phys Anthropol* **90**, 509–512.

Ravosa MJ, Simons EL (1994) Mandibular growth and function in *Archaeolemur*. *Am J Phys Anthropol* **95**, 63–76.

Ravosa MJ (1996) Mandibular form and function in North American and European Adapidae and Omomyidae. *J Morph* **229**, 171–190.

Ravosa MJ (1999) Anthropoid origins and the modern symphysis. *Folia Primatol* **70**, 65–78.

Scapino RP (1981) Morphological investigation into functions of the jaw symphysis in carnivorans. *J Morph* **167**, 339–375.

Vinyard CJ, Ravosa MJ (1998) Ontogeny, function, and scaling of the mandibular symphysis in papionin primates. *J Morph* **235**, 157–175.

Vinyard CJ, Wall CE, Williams SH, Johnson KR, Hylander WL (2006a) Masseter electromyography during chewing in ringtailed lemurs (*Lemur catta*). *Am J Phys Anthropol* **130**, 85–95.

Vinyard CJ, Williams SH, Wall CE, Johnson KR, Hylander WL (2006b) Jaw-muscle electromyography during chewing in Belanger's treeshrews (*Tupaia belangeri*). *Am J Phys Anthropol* **127**, 26–45.

Weijs WA, Hillen B (1985) Physiological cross-section of the human jaw muscles. *Acta Anat* **121**, 31–35.

Zajac FE (1989) Muscle and tendon: properties, models, scaling, and application to biomechanics and motor control. *Crit Rev Biomed Eng* **17**, 359–411.

Zhang F, Langenbach GEJ, Hannam AG, Herring SW (2001) Mass properties of the pig mandible. *J Dent Res* **80**, 327–335.